Plasma temperature of spark discharge in a spark-ignition engine using a time series of spectra measurements

N. Kawahara[1,*], S. Hashimoto[1], E. Tomita[1]
1: Dept. of Mechanical Engineering, Okayama University, Japan
* Correspondent author: kawahara@okayama-u.ac.jp

Keywords: Plasma temperature, Spark discharge, time series of emission spectra

ABSTRACT

Plasma temperature of a spark discharge was measured using a time series of emission spectra from the spark discharges. We were able to measure a time series of emission spectra from the spark discharge and initial flame kernel inside a spark-ignition engine using a spectrometer coupled with a spark plug and optical fiber. Simultaneously, high-speed visualization of spark discharge and initial flame kernel could be obtained. The plasma vibrational temperature of the spark discharge can be measured using time series emission spectra from the electrically excited CN* violet band system. The main conclusions that can be drawn from the study are as follows. CN* emission can be detected from the spark discharge, visualized using a high-speed camera during the glow discharge phase. The plasma temperature of the spark discharge is almost 5,000-6,800 K as described in Ref. 3.

1. Introduction

Combustion is initiated from the electrical spark discharge produced between the spark plug electrodes close to the end of the compression stroke in a gasoline spark-ignition engine. The high-temperature plasma kernel formed by the spark discharge and energy transfer from the high-temperature plasma to the combustible mixture occurs around the spark plug [1, 2]. The initial flame kernel created by the spark discharge becomes a propagating flame. The spark discharge process can be divided into three phases: breakdown, arc discharge, and glow discharge [3, 4]. During the breakdown phase, a highly conductive plasma channel is formed between the spark electrodes. All molecules in this spark channel are dissociated and ionized with a very high plasma electrical temperature, up to 60,000 K. The plasma electrical temperature then decreases due to plasma cooling and recombination phenomena. Ionization and dissociation energy is transformed into thermal energy during plasma cooling. In the arc phase, the thin cylindrical plasma expands, due to heat conduction and diffusion, with a lower ionization level. Due to these energy transfers, the gas temperature in the arc is limited to ~6,000 K [1, 3]. Following the arc phase, the glow discharge can be formed and maintained for several

milliseconds due to the secondary coil in a conventional coil spark-ignition system. The glow discharge has lower power but higher energy due to the long discharge time. Inside this spark channel, the combustible mixture is preheated, up to the adiabatic flame temperature. Chemical reactions are initiated by the high radical density region in the breakdown phase. After several tens of microseconds, the plasma temperature decreases, comparable to the adiabatic flame temperature. OH and CH radical emissions appears after ~100 μs due to the high energy of the glow discharge.

In this research, plasma temperature of the spark discharge was measured using a time series of spectra obtained using an electron multiplying charge-coupled device (EMCCD) spectrometer coupled with a spark plug with an optical fiber to understand the ignition process of the spark discharge in a spark-ignition engine. A spark plug with an optical fiber has been developed to obtain the emission spectra from the spark discharge and flame kernel [5]. The plasma vibrational temperature of the spark discharge was investigated using the emission spectra from the electrically excited CN violet band system [6, 7].

2. Experimental apparatus

A compression-expansion machine (CEM) with a bottom-viewed visualization system was used to visualize flame propagation in this study [8]. The CEM is equipped with a flat piston with a 78-mm bore, 85-mm stroke, 9.0 compression ratio, and a direct injection system, as shown in Figure 1. To implement a single combustion, the engine is driven by an electric motor at a constant rotational speed of 600 rpm. The CEM has one intake valve, and the exhaust gas is drawn out by a vacuum pump through the inlet valve. The intake valve is closed at bottom dead center (BDC). The mixture in the cylinder is compressed and expanded repeatedly by the piston motion. The in-cylinder pressure is measured using a pressure transducer set on the cylinder head. The intake air temperature is warmed to 363 K in a tank. Also, the cooling water temperature is warmed to 363 K.

Two kinds of fuel, propane and iso-octane, were used in this experiments. When propane was used as fuel, homogeneous mixture, propane-air mixture, was made before experiments. Initially, a homogeneous propane-air mixture was introduced into the tank and cylinder at an initial pressure P_0 through an open valve with the piston set at TDC. The engine was driven by an electric motor while the valve was kept open. After a given time, the valve was closed when the piston was located at a bottom dead center (BDC). The gas was then compressed and ignited by an electric spark at a selected crank angle θ_{IT}. On the other hand, a multi-hole injector was used for spray-guided direct injection with iso-octane at 5 MPa fuel pressure. To investigate the

radical emission from the propagating flame in the engine cylinder, the end-of-injection (EOI) timing is at crank angle 270° Before top-dead-center (BTDC) in the intake stroke as a homogeneous condition.

The developed M12-type spark plug sensor is shown in Figure 2. A demonstration picture of the spark plug sensor is also shown in Figure 2. The spark plug sensor was modified to contain an optical fiber (BFH48-1000; Thorlabs, Newton, NJ, USA) with a core diameter of 1,000 μm. It is possible to detect the light that is emitted from the flame near the spark plug during combustion. The numerical aperture (NA) of the optical fiber is 0.48, indicating the transmittable incident angle. A sapphire window that melts above 2,000°C is the optical set-up to protect the optical fiber from high pressure and temperature. The performance of the spark plug sensor was confirmed in an hour operating with wide-open throttle (WOT) at 4,000 rpm using a practical engine [5]. The light of the in-cylinder flame is led to a spectrograph (SR-303i; Andor) through the optical fiber, and is detected by an EMCCD (Newton EMCCD; Andor). To obtain chemiluminescence spectra for wavelengths in the range of 280–440 nm, a grating with 600 lines/mm was used. The wavelength resolution was 0.18 nm. A mercury-vapor lamp was used for wavelength calibration. A time series of spectra was obtained with fast kinetics mode of EMCCD. By synchronizing the gating of EMCCD with the compression-expansion machine, we were able to collect light in a time series. During these experiments, the cylinder pressure was recorded every 0.5 crank angle degree (CAD).

The combustion inside the cylinder was simultaneously visualized using a high-speed color camera (nac Image Technology, MEMRECAM GX-8) with a resolution of 128 x 128 pixels. By gating the camera so that it was in synch with the engine, we were able to acquire an image at a specific crank angle.

3. Experimental results

Figure 3 show the time series of emission spectra from the spark discharge and initial flame kernel obtained using the fiber-optic spark plug developed. The spark energy from the multiple igniter was 420 mJ, which was investigated in terms of electrical current and voltage. In this case, the glow discharge lasts until 2.0 ms after the start of the spark ignition. CN* (1, 0) and CN* (0, 0) were observed clearly at 359.0 nm and 388.3 nm from the start of the spark timing, respectively. CN* can be detected until 0.8 ms after the spark timing. The R and P branches of OH* (A-X) transition and CH* were observed clearly at 306.4 nm, 309.2 nm, and 431.4 nm, respectively, from 0.8 ms after the spark timing. OH* (A-X) can be detected until 2.8 ms after the spark timing, and CH* was detected until around 2.4 ms. CH* was formed inside the flame reaction zone of

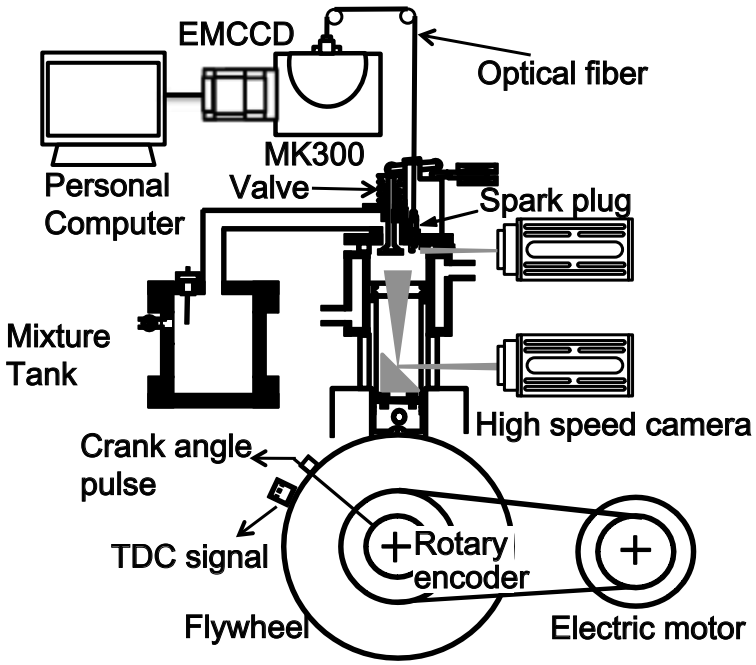

Fig. 1 Experimental set-up

Fig. 2 Spark-plug sensor with optical fiber

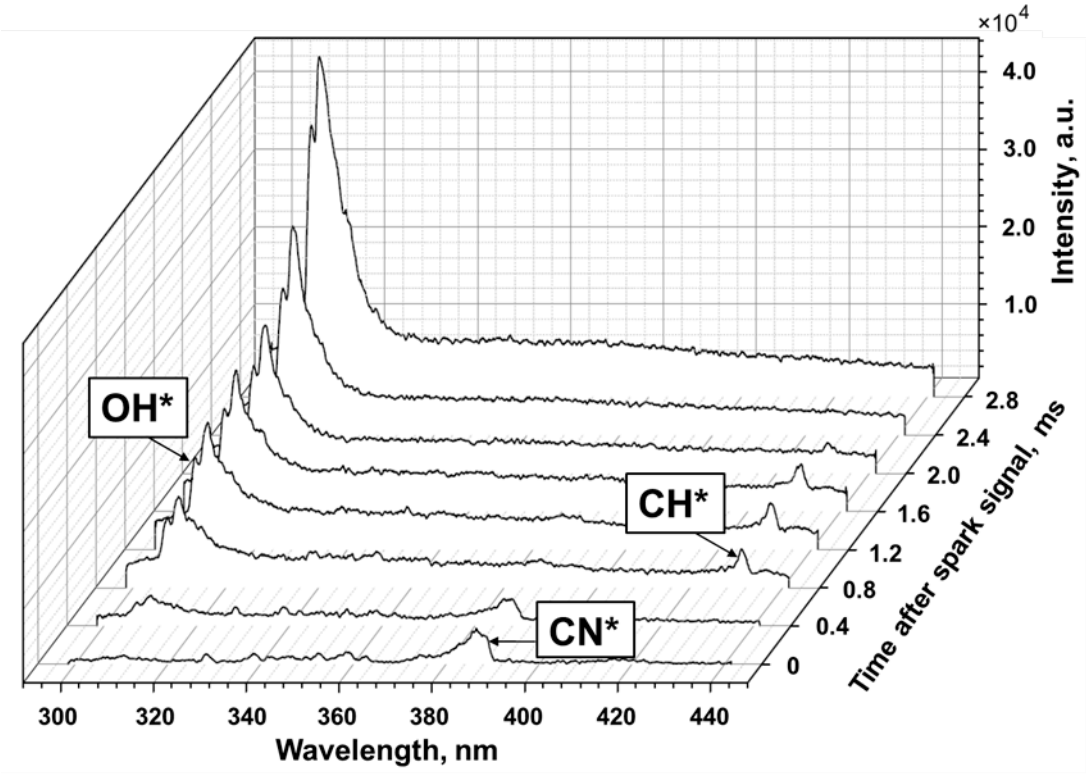

Fig. 3 Time series of emission spectra from spark discharge in a spark-ignition engine

the initial flame kernel; however, OH* (A-X) can be observed inside both of spark discharge and the burned gas region.

Figure 4 shows high-speed visualization of spark discharge and initial flame propagation of propane-air mixture. Elapsed time were shown from the start of spark discharge. Emission spectra from spark discharge between the ground and center electrodes can be visualized using high-speed color camera. When the spark discharge appears inside the NA angle of the optical fiber, CN* (1, 0) and CN* (0, 0) can be observed clearly. From the spark discharge, blue flame can be initiated from the spark discharge. OH* and CH* can be detected from the initial flame kernel from the spark discharge. Initial flame kernel is glowing as a propagating flame from the spark discharge.

The temperature of the spark discharge is important in considering the thermal energy transfer from the spark plasma to the mixture. The plasma temperature (vibrational temperature) can be evaluated using the time series of spectra. The plasma temperature (vibrational temperature) was measured using the emission spectroscopy of CN*. Figure 5 shows LIFBASE [9] simulations of CN* (0, 0) and CN* (1, 0) with changes in plasma vibrational temperature. Emission intensities were normalized to the maximum value of CN* (0, 0). When the plasma vibrational temperature increased, intensities of CN* (1, 0) increased. CN* (0, 0) and CN* (1, 0) emission spectra could be

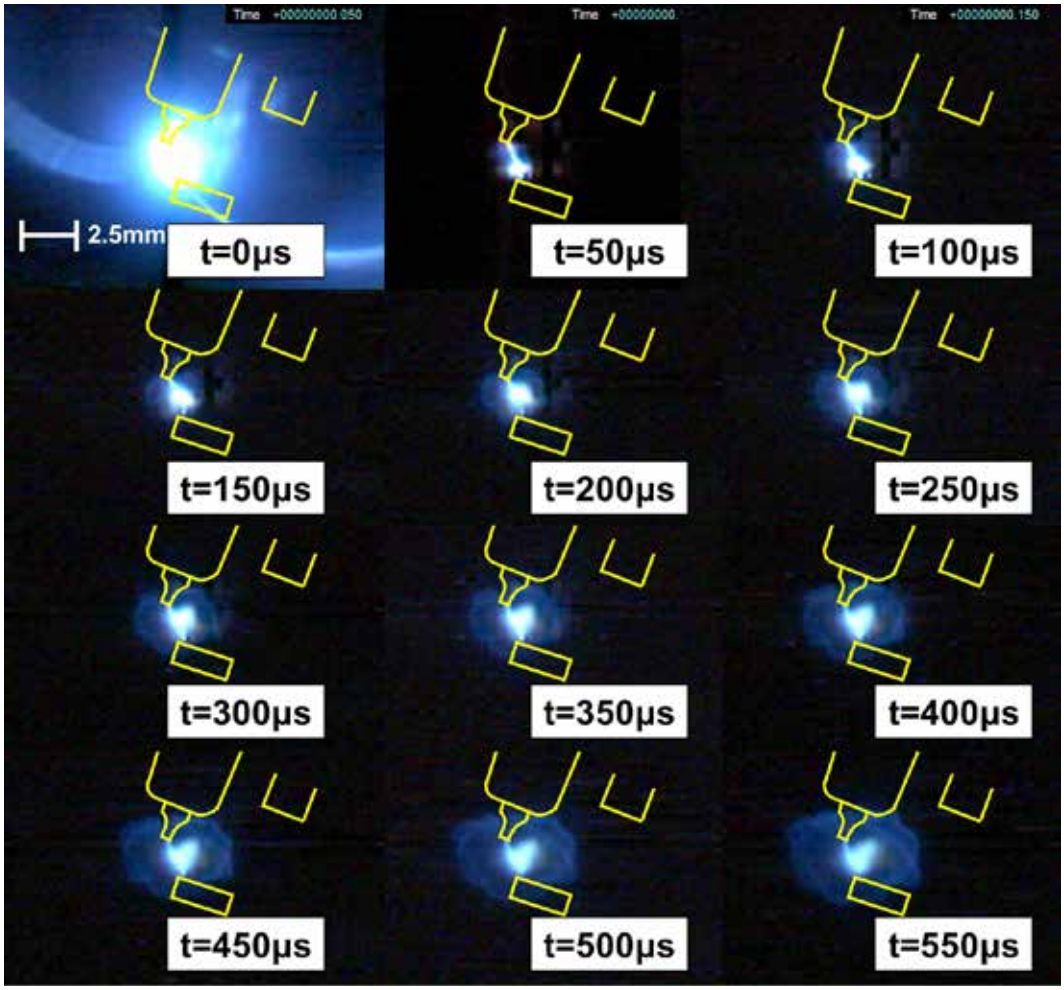

Fig. 4 High-speed visualization of spark discharge and initial flame propagation of propane-air mixture

detected in the spark discharge. Plasma vibrational temperature can be determined using the relationship between the simulated vibrational temperature and the ratio of CN* (1, 0) and CN* (0, 0) intensities. Figure 6 shows the relationship between the simulated vibrational temperature and the ratio of CN* (1, 0) and CN* (0, 0) intensities. Using this relationship, the plasma vibrational temperature can be estimated.

Figure 7 indicates the time series of plasma vibrational temperatures obtained using CN* (1, 0) and CN* (0, 0) band emissions in the case of propane-air mixture. The plasma vibrational temperature showed ~6,000 K during the glow discharge phase. After the glow discharge, CN* emission intensities decreased and the vibrational temperature could not be evaluated.

Figure 8 indicates the time series of plasma vibrational temperatures obtained using CN* (1, 0) and CN* (0, 0) band emissions in the case of iso-octane-air mixture. The plasma vibrational

temperature showed ~6,800 K during the glow discharge phase, and is almost same with propane-air mixture.

Using our optical fiber-based measurement system, we could obtain detailed information regarding the ignition process in a practical spark-ignition engine. We are going to discuss the effects of spark discharge energy to plasma vibrational temperature.

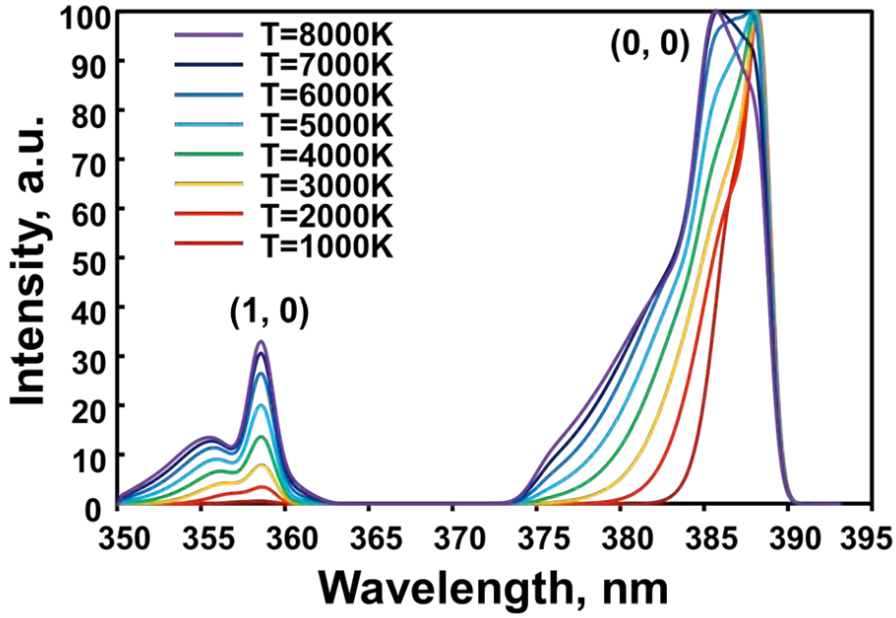

Fig. 5 Simulated CN* emission spectra

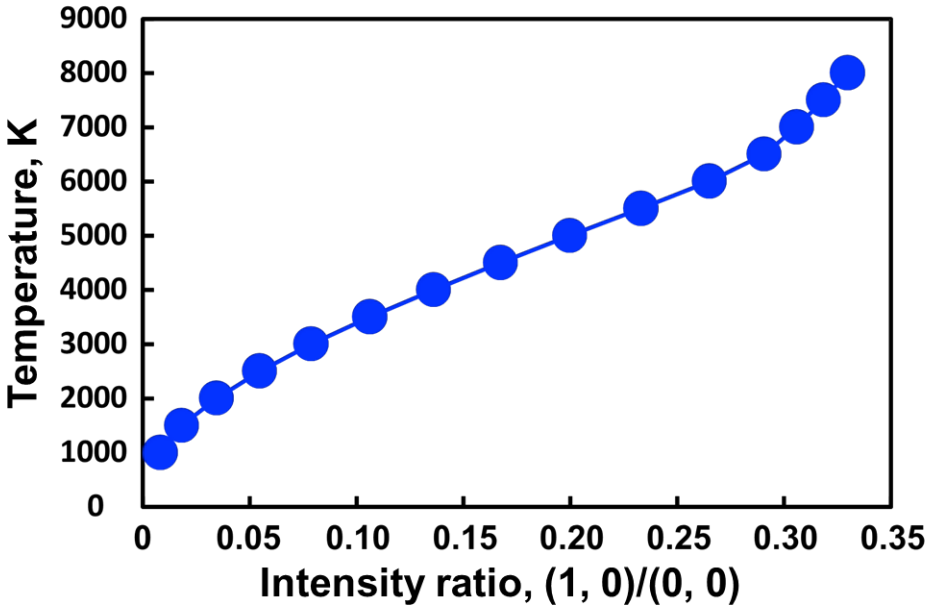

Fig. 6 Relationship between intensity ration of CN*(1, 0)/CN* (0, 0) and plasma temperature

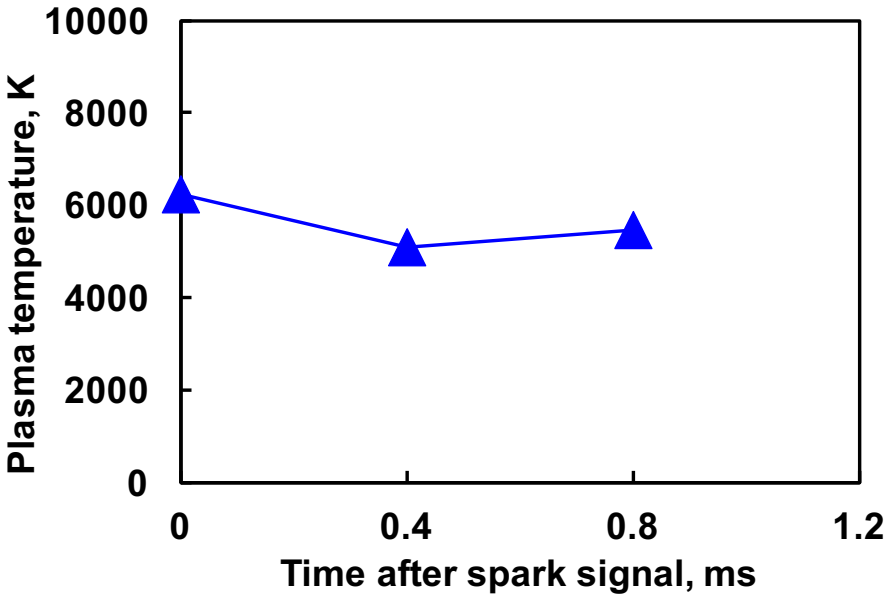

Fig. 7 Time series of plasma vibrational temperature of spark discharge in a spark-ignition engine in the case of propane-air mixture

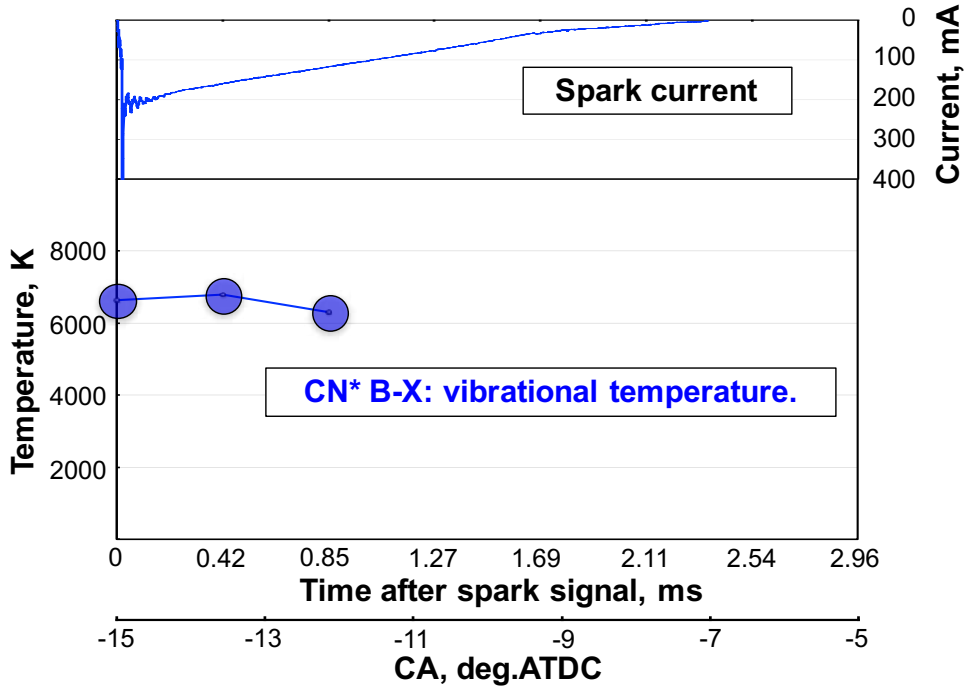

Fig. 8 Time series of plasma vibrational temperature of spark discharge in the case of iso-octane-air homogeneous mixture

Conclusions

Plasma temperature measurement of the spark discharge was carried out to understand the ignition process of the spark discharge in a spark-ignition engine using a time series of spectra obtained using an spectrometer coupled with a spark plug with optical fiber. The plasma vibrational temperature of the spark discharge can be measured using emission spectra from the electrically excited CN* violet band system. We discussed ignition process of spark discharge in a spark-ignition engine and the results obtained from this study can be summarized as follows:

1. We were able to measure a time series of emission spectra from the spark discharge and the initial flame kernel inside a spark-ignition engine. CN* emissions could be detected from the spark discharge visualized using a high-speed camera during the glow discharge phase.
2. Plasma temperature can be evaluated using the time series of emission spectra from the spark discharge inside the spark-ignition engine. The plasma temperature of the spark discharge was almost 5,000-6,800 K as described in Ref. 3.

Acknowledgments

This work was supported by Council for Science, Technology and Innovation (CSTI), Cross-ministerial Strategic Innovation Promotion Program (SIP), "Innovative Combustion Technology" (Funding agency: JST).

References

1. Heywood, J. B., Internal Combustion Engine Fundamentals, McGraw–Hill Books, Inc., (1988).
2. Stone, R, Introduction to Internal Combustion Engines, 3rd Ed., Society of Automotive Engineers, Inc, Warrendale, (1999).
3. Maly, R., and Vogel, M., Proc. Combust. Inst. 17: 821-831 (1976).
4. Herwag, R., and Maly, R., A fundamental model for flame kernel formation in S.I. engines, SAE paper No. 922243, (1992).
5. Kawahara, N., Tomita, E., Inoue, A., Time-series Spectra Measurements from Initial Flame Kernel in a Spark-Ignition Engine, 17th Int. Symp. on Application of Laser Techniques on Fluid Mechanics, session 4-7, (2014)
6. A.G. Gaydon, The Spectroscopy of Flames, Chapman and Hall, 1974.
7. Kuwahara K and Ando H (2000) Diagnostics of in-cylinder flow, mixing and combustion in gasoline engines, Measurement Science and Technology, 11: R95-R111.

8. Kawahara, N., Tomita, E., Sakata, Y., Auto-Ignited Kernels during Knocking Combustion in a Spark-Ignition Engine, Proc. of the Combust. Inst., 31, 2, (2007), pp.2999-3006.

9. Luque, J., Crosley, D. R., Database and Spectral Simulation for OH A-X, OD A-X, NO A-X, B-X, C-X, D-X, CH A-X, B-X, C-X, CN B-X, SiH A-X and CF A-X, SRI Report MP 99-009 (1999).